



Cite this: *Chem. Commun.*, 2015,
51, 11309

Received 9th April 2015,
 Accepted 4th June 2015

DOI: 10.1039/c5cc02945g

www.rsc.org/chemcomm

A zig-zag uranyl(v)–Mn(II) single chain magnet with a high relaxation barrier†

Lucile Chatelain,^{abc} Floriana Tuna,^d Jacques Pécaut^{ab} and Marinella Mazzanti*^c

The synthesis, structural characterization and magnetic properties of a 1D zig-zag coordination polymer based on a cation–cation $[(U^V O_2)Mn^{II}]$ repeated unit are reported; it shows single chain magnet (SCM) behaviour with a high energy barrier of 122 K.

Single chain magnets (SCMs) have been attracting increasing attention in the last decade¹ following the first report of slow relaxation of the magnetization in a 1 D coordination polymer.² Notably SCMs provide an attractive alternative to 0 D molecular magnets (SMMs) for the development of information storage devices.^{1a,3} The requirements to observe the SCM behaviour first predicted by Glauber⁴ are the presence of strong Ising anisotropy, high intra-chain magnetic coupling and weak inter-chain interactions. Notably, the high anisotropy of 5d and 4f ions has been successfully exploited to afford 1 D coordination polymers with SCM behaviour.^{5,6}

Actinide ions have been recently attracting increasing attention for the design of SMMs due to their high anisotropy and their ability to engage in strong magnetic exchange.^{7,8} However only one example of an actinide based single chain magnet has been reported so far.⁹

Our group and others have demonstrated that cation–cation interactions (described as the bonding of an actinyl imido or an oxo group with a metal cation) provide a convenient route to magnetic exchange^{7j,m,8b,9,10} and to the assembly of exchange-coupled SMMs.^{7j,m,8b,9} In particular, we have recently shown that, depending on the reaction stoichiometry, the cation–cation interaction between the uranyl(v) $[UO_2(salen)(Py)]^-$

building block and the $[Mn(II)(Py)_n]$ unit leads either to a $\{U_{12}Mn_6\}$ wheel-shaped uranyl(v) cluster with SMM behaviour^{7m} or to a linear 1 D polymer with a SCM behaviour.⁹

Here we report the first actinide based 1D zig-zag coordination polymer $\{[UO_2(\text{Mesaldien})][Mn(NO_3)(Py)_2]\}_n$, **2**, that is built from the cation–cation interaction of the uranyl(v) complex $[UO_2(\text{aldien})]^-$ with $[Mn(II)(NO_3)(Py)_2]$. Polymer **2** shows slow relaxation of the magnetization with a high relaxation barrier of 122 K and an open magnetic hysteresis loop at $T < 3$ K, with a coercive field of 1.75 T at 2 K. Compound **2** is thus only the second example of an actinide based polymer showing SCM behaviour which most likely arises from a strong intra-chain coupling combined with the high Ising anisotropy of the uranyl(v) dioxo group.

The monomeric uranyl(v) complex $[UO_2(\text{Mesaldien})][Cp^*_2Co]$, **1**, containing the pentadentate Schiff base Mesaldien was prepared in high yield (90%) by reduction of the analogous monomeric uranyl(vi) complex with one equivalent of Cp^*_2Co in pyridine (see the ESI†). Complex **1** is fully stable in the solid state and in a variety of organic solvents. The stability of complex **1** with respect to the disproportionation reaction is consistent with previously reported spectroscopic and synthetic studies showing that pentadentate Schiff bases stabilize pentavalent uranyl by saturating the equatorial coordination sites and therefore preventing the formation of dimeric disproportionation intermediates.^{11a–c} As such complex **1** provides an excellent precursor for the controlled synthesis of heteropolymetallic cation–cation assemblies. Notably, the reaction of **1** with one equivalent of the $Mn(NO_3)_2$ salt affords the 1D polymer $\{[UO_2(\text{Mesaldien})][Mn(NO_3)(Py)_2]\}_n$, **2**, as a pink microcrystalline powder in 66% yield (Scheme 1). The X-ray crystal structure of **2** is shown in Fig. 1.

In the structure of **2** the oxo groups of the uranyl(v), $[UO_2(\text{Mesaldien})]^-$ units bridge through a linear cation–cation interaction between two $[Mn(NO_3)(Py)_2]^+$ cations to yield a zig-zag one-dimensional chain. The asymmetric unit of **2** contains only one uranium and one manganese atoms forming the neutral repeated entity $\{[UO_2(\text{Mesaldien})][Mn(NO_3)(Py)_2]\}$. The uranium atom is heptacoordinated with a slightly distorted pentagonal

^a Univ. Grenoble Alpes, INAC-SCIB, F-38000 Grenoble, France

^b CEA, INAC-SCIB, F-38000 Grenoble, France

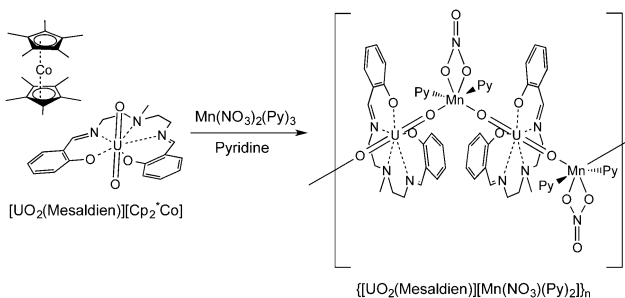
^c Institut des Sciences et Ingénierie Chimiques, Ecole Polytechnique Fédérale de Lausanne (EPFL), CH-1015 Lausanne, Switzerland.

E-mail: marinella.mazzanti@epfl.ch

^d School of Chemistry and Photon Science Institute, University of Manchester, Oxford Road, Manchester, M13 9PL, UK

† Electronic supplementary information (ESI) available. CCDC 1058487 and 1058488. For ESI and crystallographic data in CIF or other electronic format see DOI: 10.1039/c5cc02945g





Scheme 1 Synthesis of **2**.

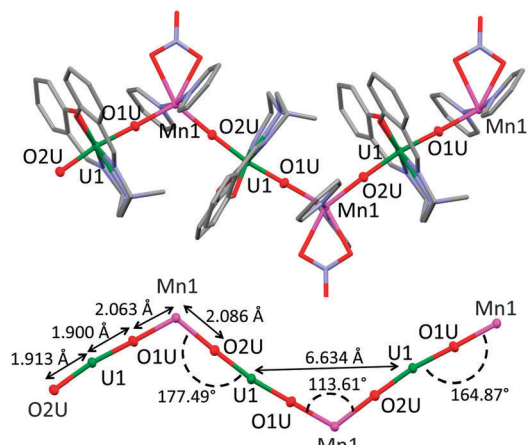


Fig. 1 Mercury view of the structure of **2** (top) and enhanced view of the zig-zag core with associated distances and angles. (bottom) (Ligands were represented in pipes, H and co-crystallised solvent molecules were omitted for clarity, C is represented in grey, O in red, N in light blue, Mn in pink and U in green).

bipyramidal geometry by the five donor atoms of the Mesaldien ligand situated in the equatorial plane and by the two uranyl oxygens in the axial position. The manganese(II) ion is hexa-coordinated, by two uranyl oxygens from two different uranyl(V) units, two pyridines and the two oxygens of the bidentate nitrate ligand. Due to the $\text{U(V)O}_2\text{-Mn(II)}$ cation-cation interactions, the U=O bond distances are lengthened (U1-O1U 1.900(3) Å and U1-O2U 1.913(3) Å) compared to those found in $[\text{UO}_2(\text{Mesaldien})][\text{Cp}^*_2\text{Co}]$ 1 (U1-O1U 1.847(6) Å and U1-O2U 1.846(6) Å). The mean Mn-O_{yl} (where O_{yl} is the uranyl oxygen) bond distance in 2 is 2.075(3) Å, significantly shorter than that found in the $\{\text{U}_{12}\text{Mn}_6\}$ wheel-shaped uranyl(V) cluster^{7m} (2.15(2) Å) but similar to that found in a trinuclear $[\text{U(V)O}_2\text{Mn(II)}_2]$ complex (2.055(6) Å).^{8b} The U-O-Mn angles deviate slightly from linearity and range from 164.87° to 177.49°. The asymmetric unit is repeated thanks to a 2-fold screw axis along the 0, y, 1/4 direction resulting in a zig-zag topology with a U-Mn-U angle of 113.61°. The observed geometry is very different from that observed for the only other reported uranium based SCM $\{[\text{UO}_2(\text{salen})(\text{Py})][\text{Mn}(\text{Py})_4]\text{NO}_3\}_n$,⁹ assembled from the uranyl(V) complex of the tetridentate Schiff base salen, where the mean U-M-U angle is practically linear (170.25°). The deviation from linearity probably results from the presence of a bidentate nitrate ligand bonded to the manganese cation.

An intra-chain separation between neighbouring U(v) ions of 6.634 Å and a separation between neighbouring Mn(II) ions of 7.897 Å are found in 2 whereas the mean intramolecular U–Mn distance is 3.96(3) Å. Each chain is separated from the nearest chain with a minimum intermetallic distance of 11.881, 10.336 and 9.019 Å, respectively, for U–U, U–Mn and Mn–Mn. No significant interchain π -stacking is observed in the structure of 2.

Magnetic susceptibility measurements were performed first between 2 and 300 K on a polycrystalline sample of **2** at magnetic fields of 0.01, 0.1, 0.5 and 5 T (see the ESI†). The measured χT value for **2** at room temperature is approximately $4.8 \text{ cm}^3 \text{ K mol}^{-1}$ which is consistent with the values reported for heteropolymetallic Mn(II)-uranyl(V) assemblies containing one spin-only divalent manganese (with $S = 5/2$ and g close to 2) and one pentavalent uranium ion.⁹ The χT product remains constant from 300 K to 80 K before reaching a field-dependent maximum ($177.8 \text{ cm}^3 \text{ K mol}^{-1}$ at 0.01 T, $77.29 \text{ cm}^3 \text{ K mol}^{-1}$ at 0.1 T, $26.3 \text{ cm}^3 \text{ K mol}^{-1}$ at 0.5 T; $6.7 \text{ cm}^3 \text{ K mol}^{-1}$ at 5 T). At very low temperatures this product drops rapidly probably due to saturation effects, magnetic anisotropy and/or inter-chain anti-ferromagnetic interactions. The increase of χT below 80 K suggests the presence of a dominant ferromagnetic interaction leading to an aligned-spin ground state.

The scaling of the χT data of **2** (Fig. 2, left) clearly shows the occurrence of a linear regime characteristic of Ising 1D systems. The $\ln(\chi T)$ versus $1/T$ plot increases linearly between 45 and 16 K ($1/T$ from 0.063 to 0.022 K $^{-1}$). The experimental data were fitted within this linear regime using the equation $\chi T = C_{\text{eff}} \exp(\Delta/k_B T)$ which describes a ferromagnetically coupled infinite chain. The fit gives an energy gap Δ/k_B of 43.4 K and a pre-exponential factor $C_{\text{eff}} = 2.50$. The magnetic susceptibility data of **2** between 16 and 300 K at 0.01 T were also fitted with the equation $\chi T = C_1 \exp(\Delta_1/k_B T) + C_2 \exp(\Delta_2/k_B T)$, where a second negative exponential is added to take into account the high-temperature crystal field effect and possible antiferromagnetic

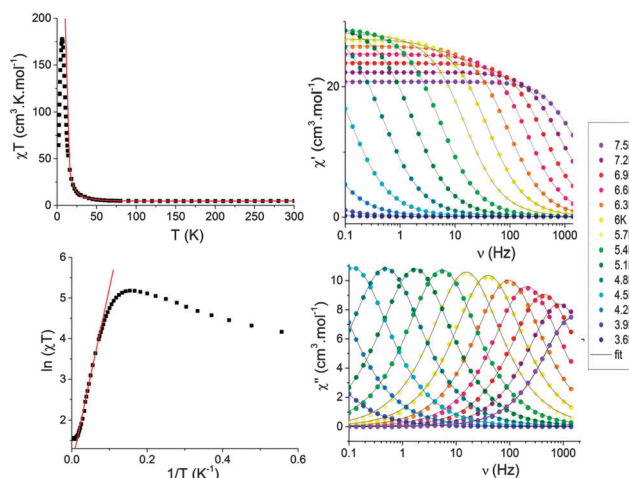


Fig. 2 Left: plots of (top) χT versus T and (bottom) $\ln(\chi T)$ versus $1/T$ for a polycrystalline sample of **2**, measured at 0.01 T applied field. Right: temperature dependence of the (top) real (χ') and (bottom) imaginary (χ'') ac susceptibilities for **2** measured at zero-dc field and 1.5 G ac field.

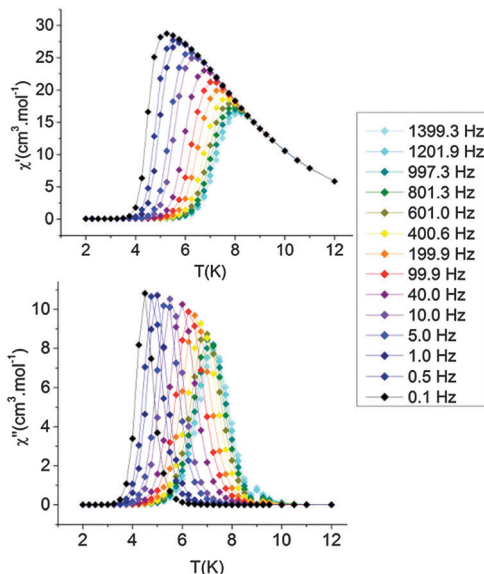


Fig. 3 Frequency dependence of the (top) real (χ') and (bottom) imaginary (χ'') ac susceptibilities for **2** measured at zero-dc field and an ac field of 1.5 oscillating at frequencies between 0.1 and 1400 Hz.

contributions. In this case we obtained $\Delta_1/k_B = 44.1$ K, $\Delta_2/k_B = -107.8 \pm 10.5$ K, $C_1 = 2.43 \text{ cm}^3 \text{ K mol}^{-1}$, and $C_2 = 2.80 \text{ cm}^3 \text{ K mol}^{-1}$, in very good agreement with the previous considerations. The high-temperature extrapolated Curie constant, $C = C_1 + C_2 = 5.23 \text{ cm}^3 \text{ K mol}^{-1}$, is close to the expected value for one Mn(II) and one U(V) ions.

Isothermal variable-field (-7 T to $+7$ T) magnetisation measurements were then performed at several temperatures between 2 and 5 K (Fig. 4). These measurements reveal an open hysteresis cycle below 3 K. This result confirms the existence of a magnetic ground state in **2** and the presence of a magnetic bistability. A significant coercive field of 1.75 T is obtained at 2 K, which decreases with increasing temperatures. A divergence between field cooled and zero field cooled magnetisations as a function of temperature is observed below 3 K and a remanent magnetisation (REM) of $2.2 \mu_B$ is preserved at very low temperatures under zero field before vanishing after 3 K. These features suggest that this material behaves like a single chain magnet with a blocking temperature $T_B = 3$ K. The blocking temperature of **2** is significantly smaller than that reported for the linear chain $\{[\text{UO}_2(\text{salen})(\text{Py})][\text{Mn}(\text{Py})_4]\text{NO}_3\}_n$ (5.8 K) highlighting the effect of the zig-zag geometry and of the ligand coordinated to the uranyl(V) on the magnetic properties.

The dynamic magnetisation was investigated to probe magnetic relaxation in **2**. Zero-field ac susceptibility measurements between 3.6 and 7.5 K were carried out at several frequencies between 0.1 and 1399 Hz with a 1.55 G ac field (Fig. 2 right). Both the in-phase (χ') and out-of-phase (χ'') components of the ac susceptibility show strong frequency dependence below *ca.* 7.5 K; maxima are observed in $\chi''(T)$ (Fig. 3). This result rules out the presence of any tridimensional ordering. Moreover, the value of the parameter $\phi = (\Delta T_{\max}/T_{\max})/\Delta(\log f) \approx 0.10$, measuring the relative variation of the temperature of the

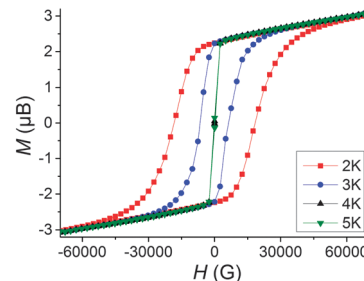


Fig. 4 Field dependence of the magnetisation of **2** measured at four different temperatures with a field sweep rate of 0.0061 T.s^{-1} .

maximum of $\chi''(T)$ with respect to the frequency, is in the range of normal superparamagnets and excludes the possible occurrence of a spin glass state.¹²

The frequency dependence of the in-phase (χ') and out-of-phase (χ'') components of the ac susceptibility was fitted to a generalized Debye model for one relaxation process with the α parameter in the range of 0.11–0.20 revealing a narrow distribution of relaxation times. Semi-circular Cole–Cole plots (χ'' vs. χ') are obtained for temperatures below 7.2 K confirming that only one relaxation process occurs. Both ac experiments as a function of frequency or temperature allow the determination of relaxation times and they were fitted to the Arrhenius equation $\tau = \tau_0 \exp(U/k_B T)$, where τ is the relaxation time, $U_1 = 122.1(14)$ K is the energy barrier for the relaxation of the magnetisation and $\tau_0^{(1)} = 6.2 \times 10^{-12}$ s is the pre-exponential factor (Fig. S9, ESI†). A crossing in the Arrhenius plot occurs, giving a second energy barrier of $U_2 = 107.0(7)$ K associated with $\tau_0^{(2)} = 7.4 \times 10^{-11}$ s. This value must be regarded with caution because of the limited T -range over which the relaxation times were determined. Several SCM systems were reported to show two activated regions due to finite-size effects.¹ Thus, the energy barrier of the zig-zag chain is very high and only moderately smaller than for the previously reported U(V)Mn(II) linear chain (134.0(8) K).⁹ The high relaxation barrier of the zig-zag chain is most likely the result of the ferromagnetic intra-chain coupling associated with the large anisotropy from the strong Ising-type ligand field of the uranyl group.¹³

In conclusion we have shown that the cation–cation assembly of the uranyl(V) complex of a pentadentate Schiff base ligand with the $[\text{Mn}(\text{II})(\text{NO}_3)(\text{Py})_2]$ unit affords a 5f–3d heterometallic 1D chain with a novel zig-zag topology. The presented results show that different chain topologies can be obtained just by changing the nature of the Schiff base ligand in the uranyl(V) building block. Variable-temperature dc magnetic susceptibility measurements demonstrate the presence of intrachain ferromagnetic exchange coupling within the chain. Moreover, this zig-zag 1D polymer shows SCM behaviour with a high relaxation barrier and an open magnetic hysteresis affording the second example of actinide based SCM so far isolated. The high stability of the $[\text{UO}_2(\text{Mesaldien})]^-$ building block provides a versatile route to a wide variety of 3d–5f 1D chains that will be investigated in future studies.

Notes and references

1 (a) W. X. Zhang, R. Ishikawa, B. Breedlove and M. Yamashita, *RSC Adv.*, 2013, **3**, 3772–3798; (b) H. L. Sun, Z. M. Wang and S. Gao, *Coord. Chem. Rev.*, 2010, **254**, 1081–1100; (c) H. Miyasaka, M. Julve, M. Yamashita and R. Clerac, *Inorg. Chem.*, 2009, **48**, 3420–3437; (d) S. W. Przybylak, F. Tuna, S. J. Teat and R. E. P. Winpenny, *Chem. Commun.*, 2008, 1983–1985.

2 (a) A. Caneschi, D. Gatteschi, N. Lalioti, C. Sangregorio, R. Sessoli, G. Venturi, A. Vindigni, A. Rettori, M. G. Pini and M. A. Novak, *Angew. Chem., Int. Ed.*, 2001, **40**, 1760–1763; (b) R. Clerac, H. Miyasaka, M. Yamashita and C. Coulon, *J. Am. Chem. Soc.*, 2002, **124**, 12837–12844.

3 D. Gatteschi, R. Sessoli and J. Villain, *Molecular Nanomagnets*, Oxford University Press, Oxford, UK, 2006.

4 R. J. Glauber, *J. Math. Phys.*, 1963, **4**, 294–307.

5 (a) E. V. Peresypkina, A. M. Majcher, M. Rams and K. E. Vostrikova, *Chem. Commun.*, 2014, **50**, 7150–7153; (b) T. D. Harris, M. V. Bennett, R. Clerac and J. R. Long, *J. Am. Chem. Soc.*, 2010, **132**, 3980–3988.

6 (a) K. Bernot, L. Bogani, A. Caneschi, D. Gatteschi and R. Sessoli, *J. Am. Chem. Soc.*, 2006, **128**, 7947–7956; (b) R. Sessoli and A. K. Powell, *Coord. Chem. Rev.*, 2009, **253**, 2328–2341; (c) Y. Z. Zheng, Y. H. Lan, W. Wernsdorfer, C. E. Anson and A. K. Powell, *Chem. – Eur. J.*, 2009, **15**, 12566–12570.

7 (a) J. R. Long and K. R. Meihaus, *J. Chem. Soc., Dalton Trans.*, 2015, **44**, 2517–2528; (b) N. Magnani, *Int. J. Quantum Chem.*, 2014, **114**, 755–759; (c) K. R. Meihaus, S. G. Minasian, W. W. Lukens, Jr., S. A. Koizmor, D. K. Shuh, T. Tyliszczak and J. R. Long, *J. Am. Chem. Soc.*, 2014, **136**, 6056–6068; (d) J. D. Rinehart, K. R. Meihaus and J. R. Long, *J. Am. Chem. Soc.*, 2010, **132**, 7572–7573; (e) J. D. Rinehart and J. R. Long, *J. Am. Chem. Soc.*, 2009, **131**, 12558–12559; (f) M. A. Antunes, L. C. J. Pereira, I. C. Santos, M. Mazzanti, J. Marcalo and M. Almeida, *Inorg. Chem.*, 2011, **50**, 9915–9917; (g) J. T. Coutinho, M. A. Antunes, L. C. J. Pereira, H. Bolvin, J. Marcalo, M. Mazzanti and M. Almeida, *J. Chem. Soc., Dalton Trans.*, 2012, **41**, 13568–13571; (h) L. C. J. Pereira, C. Camp, J. T. Coutinho, L. Chatelain, P. Maldivi, M. Almeida and M. Mazzanti, *Inorg. Chem.*, 2014, **53**, 11809–11811; (i) N. Magnani, C. Apostolidis, A. Morgenstern, E. Colineau, J. C. Griveau, H. Bolvin, O. Walter and R. Caciuffo, *Angew. Chem., Int. Ed.*, 2011, **50**, 1696–1698; (j) N. Magnani, E. Colineau, R. Eloirdi, J. C. Griveau, R. Caciuffo, S. M. Cornet, I. May, C. A. Sharrad, D. Collison and R. E. P. Winpenny, *Phys. Rev. Lett.*, 2010, **104**, 197202; (k) N. Magnani, E. Colineau, J. C. Griveau, C. Apostolidis, O. Walter and R. Caciuffo, *Chem. Commun.*, 2014, **50**, 8171–8173; (l) S. Carretta, G. Amoretti, P. Santini, V. Mougel, M. Mazzanti, S. Gambarelli, E. Colineau and R. Caciuffo, *J. Phys.: Condens. Matter*, 2013, **25**, 486001; (m) V. Mougel, L. Chatelain, J. Pecaut, R. Caciuffo, E. Colineau, J. C. Griveau and M. Mazzanti, *Nat. Chem.*, 2012, **4**, 1011–1017; (n) D. P. Mills, F. Moro, J. McMaster, J. van Slageren, W. Lewis, A. J. Blake and S. T. Liddle, *Nat. Chem.*, 2011, **3**, 454–460; (o) D. M. King, F. Tuna, J. McMaster, W. Lewis, A. J. Blake, E. J. L. McInnes and S. T. Liddle, *Angew. Chem., Int. Ed.*, 2013, **52**, 4921–4924.

8 (a) F. Moro, D. P. Mills, S. T. Liddle and J. Slangeren, *Angew. Chem., Int. Ed.*, 2013, **52**, 1–5; (b) L. Chatelain, J. P. S. Walsh, J. Pecaut, F. Tuna and M. Mazzanti, *Angew. Chem., Int. Ed.*, 2014, **53**, 13434–13438.

9 V. Mougel, L. Chatelain, J. Hermle, R. Caciuffo, E. Colineau, F. Tuna, N. Magnani, A. de Geyer, J. Pecaut and M. Mazzanti, *Angew. Chem., Int. Ed.*, 2014, **53**, 819–823.

10 (a) P. L. Arnold, E. Hollis, G. S. Nichol, J. B. Love, J. C. Griveau, R. Caciuffo, N. Magnani, L. Maron, L. Castro, A. Yahia, S. O. Odoh and G. Schreckenbach, *J. Am. Chem. Soc.*, 2013, **135**, 3841–3854; (b) P. L. Arnold, E. Hollis, F. J. White, N. Magnani, R. Caciuffo and J. B. Love, *Angew. Chem., Int. Ed.*, 2011, **50**, 887–890; (c) L. Chatelain, V. Mougel, J. Pecaut and M. Mazzanti, *Chem. Sci.*, 2012, **3**, 1075–1079; (d) V. Mougel, P. Horeglad, G. Nocton, J. Pecaut and M. Mazzanti, *Angew. Chem., Int. Ed.*, 2009, **48**, 8477–8480; (e) G. Nocton, P. Horeglad, J. Pecaut and M. Mazzanti, *J. Am. Chem. Soc.*, 2008, **130**, 16633–16645; (f) L. P. Spencer, E. J. Schelter, P. Yang, R. L. Gdula, B. L. Scott, J. D. Thompson, J. L. Kiplinger, E. R. Batista and J. M. Boncella, *Angew. Chem., Int. Ed.*, 2009, **48**, 3795–3798.

11 (a) K. Takao, M. Kato, S. Takao, A. Nagasawa, G. Bernhard, C. Hennig and Y. Ikeda, *Inorg. Chem.*, 2010, **49**, 2349–2359; (b) K. Takao, S. Tushima, S. Takao, A. C. Scheinost, G. Bernhard, Y. Ikeda and C. Hennig, *Inorg. Chem.*, 2009, **48**, 9602–9604; (c) V. Mougel, J. Pecaut and M. Mazzanti, *Chem. Commun.*, 2012, **48**, 868–870.

12 J. A. Mydosh, *Spin Glasses: An Experimental Introduction*, Taylor and Francis, London, 1993.

13 G. Nocton, P. Horeglad, V. Vetere, J. Pecaut, L. Dubois, P. Maldivi, N. M. Edelstein and M. Mazzanti, *J. Am. Chem. Soc.*, 2010, **132**, 495–508.

